Intramolecular charge transfer dual fluorescent sensors from 4-(dialkylamino)benzanilides with metal binding site within electron acceptor

Li-Hong Liu,[a] Han Zhang,[a] Ai-Fang Li,[a] Jian-Wei Xie[b] and Yun-Bao Jiang[a,*]

[a]Department of Chemistry and The Key Laboratory of Analytical Sciences of the Ministry of Education,
College of Chemistry and Chemical Engineering, Xiamen University, Xiamen 361005, China
[b]Institute of Pharmacology and Toxicology, Beijing 100850, China

Abstract—Three fluoroionophores (**2a–c**) were designed as the intramolecular charge transfer (CT) dual fluorescent sensors for metal cations with metal binding site within the electron acceptor. These sensors were derived from 4-dialkylaminobenzanilides (alkyl=methyl, ethyl, and *n*-butyl) with the amido phenyl ring being an arm of 15-crown-5 thus bearing binding site for alkaline and alkaline earth metal cations. Compounds **2a–c** were expected to have two possible CT channels of opposite direction. The absorption and fluorescence spectra of **2a–c** and their crown-ether free model molecules **3a–c** in a variety of solvents were recorded. Dual fluorescence was observed with **2a–c** and was assigned to the LE and the CT states, respectively. In nonpolar or less polar solvents the CT occurring with **2a–c** was identified as that occurred with benzanilides (BA) with the amido anilines being the electron donor (the BA-like CT), while in polar solvents such as acetonitrile (ACN), the CT was still mainly the BA-like. In the presence of alkali and alkaline earth metal cations in ACN, the CT dual fluorescence underwent substantial changes so as increased total quantum yield, red-shifted LE band and enhanced CT to LE intensity ratio. Binding of the metal cations at the 15-crown-5 moiety of **2a–c** was shown to turn the CT direction that the dialkylamino group in the binding complexes being the electron donor while the benzo-15-crown-5 moiety now being within the electron acceptor. The occurrence of this CT enhances metal cation binding to 15-crown-5 ether in **2a–c**, which was confirmed by the observed higher metal binding constants. Compounds **2a–c** as the CT dual fluorescent sensors were shown to operate under the mechanism of the metal cation binding induced switching of the CT character from the BA-like to that occurred with 4-(dimethylamino)benzamides (the DMABA-like). Compounds **2a–c** therefore represent successful examples for the CT dual fluorescent sensors for cations with the metal binding site within the electron acceptor and can be employed as sensitive ratiometric fluorescent sensors for metal cations of improved sensing performance.
© 2006 Published by Elsevier Ltd.

1. Introduction

It is known that the excited-state intramolecular charge transfer (CT) and the accompanied dual fluorescence of the electron donor/acceptor substituted benzenes, such as 4-(dimethylamino)benzonitrile (DMABN), depend sensitively on the nature of the electron donor/acceptor.[1] Therefore it is possible to design fluorescent sensors for metal cation sensing. The dependence on the electron donor has been nicely supported by the effect of metal cation on the CT emission of DMABN derivatives with their amino nitrogen atom being incorporated in an aza-crown ether and employed to construct CT fluorescent sensors for metal cations.[2] Research, however, showed that there was a de-coordination reaction in the excited metal–complexes of these DMABN derivatives as a consequence of the CT process in the DMABN derivatives, where a shift of the negative

charge from the amino electron donor to the acceptor leads to an electrostatic repulsion between the metal cation and the positively charged donor.[3] The fluorescence emission, therefore, experiences relatively small changes in both its intensity and position because most of the fluorescence is emitted from the species in which the interaction between metal cation and the fluorescent sensor is much weaker or does not exist any more. It was hence expected that a similar strategy applied to the electron acceptor might lead to a better sensing performance since in this case the excited-state CT might enhance the binding of metal cations. Efforts have been made to prepare the derivatives of 4-(dimethylamino)-benzamide (DMABA) and 4-(dimethylamino)benzene-sulfonamide (DMASA) of which the amido or sulfonamido nitrogen atoms in the electron acceptor are incorporated within a metal cation binding site.[4] It turned to be not straightforward to show the expected advantage, since metal-cation binding resulted in a breakdown of the electronic conjugation in DMABA derivatives of their amido

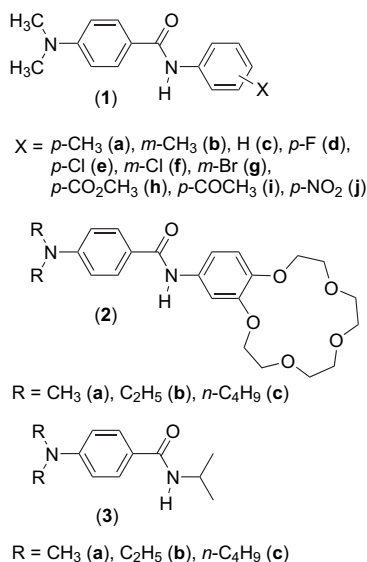* Corresponding author. E-mail: ybjiang@xmu.edu.cn

Chart 1. Molecular structures of 4-dimethylaminobenzalinides (**1**)[5] and related fluoroionophores (**2**) as metal cation sensors and their model molecules (**3**).

nitrogen with the benzoyl π-system due to steric reasons[4a] or deprotonation of the sulfonamido –NH proton.[4b] It hence remains a challenge to devise dual fluorescent CT sensors for metal cation with the electron acceptors bearing an ion binding site. The dual emission character makes these efforts worthwhile since ratiometric fluoroionophores might be constructed.

We recently investigated the intramolecular CT of a series of dual fluorescent 4-(dimethylamino)benzanilides bearing a *para*- or *meta*-substituent at the amido phenyl ring (**1**, Chart 1).[5] We showed that with **1** there existed two competitive CT channels, one from the 4-dimethylamino donor to the benzamide moiety as what was assigned for 4-(dimethylamino)benzamide[6] (the DMABA-like CT), and the other from the amido aniline to benzoyl as was shown with benzanilides[7] (the BA-like CT). It was found[5] that electron-withdrawing substituents at the amido phenyl ring in **1** could switch the excited-state CT from the BA-like to the DMABA-like. In the latter case the benzanilide moiety in **1** becomes electron acceptor. This might open up a new way of constructing CT dual fluorescent sensors for metal cations with the cation binding site within the electron acceptor while the steric influence previously encountered[4]

can be efficiently avoided,[8] as now the metal binding site is away from the amido –C(O)NH– moiety while the metal binding message can be efficiently delivered via the amido phenyl π-moiety.

We report herein our proof-of-principle effort in regard to the three derivatives of 4-(dialkylamino)benzanilide with the amido phenyl ring being an arm of 15-crown-5, known as a good macrocycle for alkaline and alkaline earth metal cations, while alkyl is methyl, ethyl, and *n*-butyl, respectively (**2a–c**, Chart 1). Compounds **2a–c** and their crown-ether free model molecules **3a–c** were synthesized according to procedures depicted in Scheme 1. Compounds **2a**, **2b**, and **2c** have similar structure, differing only at the 4-amino alkyl substituent that was expected to tune the contribution of the DMABA-like CT in which the 4-dialkylamino group acts as the electron donor.[9] As 4-dialkylamine and amido aniline in **2a–c** can function as the electron donor of the DMABA- and BA-like CT, respectively, the present CT fluorescent sensors represent a new set of D–A–D′ molecular patterns.[10] Model molecules **3a–c** were designed to help understanding the CT character of **2a–c**, since they were assumed to have similar steric structure to that of **2a–c** at the amide conjunction, but have only the DMABA-like CT channel. It was expected that, upon cation complexation to the crown-ether group in **2a–c**, the 15-crown-5 ether moiety, taken as a substituent at the amido aniline moiety of **1** (Chart 1), might become less electron donating or even electron withdrawing. The DMABA-like CT reaction channel in **2a–c** would hence predominate over the BA-like CT, resulting in a detectable change in its dual fluorescence. In this article we will show that the CT with **2a–c** is switched from the BA-like to the DMABA-like when metal cation is bound to the crown-ether group, allowing hence for the CT dual fluorescent sensing of metal cations with the cation-binding site locating within the electron acceptor.

2. Results and discussion

2.1. 15-Crown-5 group as a 'substituent' in 2a–c

Previously we showed that substituent in **1** (Chart 1) at the *para*- or *meta*-position of the amido aniline did not affect the ground-state structure of **1**, in particular at the amide conjunction.[5] Actually a linear correlation was found between the ^{1}H NMR chemical shift of the amido –NH proton (δ_{-NH}, ppm) of **1** in DMSO-d_6 and the Hammett
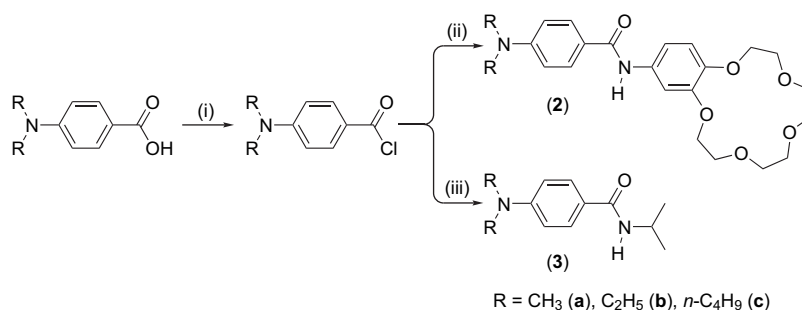
Scheme 1. Syntheses of **2** and **3**. Reagents and conditions: (i) SOCl$_2$ (3 equiv), CH$_2$Cl$_2$, rt; (ii) 4-aminobenzo-15-crown-5 ether hydrochloride (1 equiv), NEt$_3$ (1.2 equiv), CH$_2$Cl$_2$, rt and (iii) *iso*-propylamine (1 equiv), CH$_2$Cl$_2$, rt.

substituent constant (σ_x), $\delta_{-NH}=0.66\sigma_x+9.84$. It is therefore possible to construct metal cation fluorescent sensors by incorporating a cation binding site, such as crown-ether, in the amido aniline at its *para-* and/or *meta-*positions. In this case metal binding would hardly introduce any steric hindrance to the amido conjunction. This was the basis for our design of **2a–c** as the metal cation sensors. Obviously the 15-crown-5 group in **2a–c**, a substituent at the amido aniline moiety in **1**, could be approximately taken as a *p*-OEt plus an *m*-OEt, and is therefore electron donating. On the basis of the chemical shift of the amido –NH proton of **2a** (9.722 ppm),[11] the 'substituent' constant of the 15-crown-5 group in **2a** was calculated from the aforementioned linear relationship to be −0.18, which is indeed close to the sum of the Hammett constants of *p*-OEt ($\sigma=-0.24$) and *m*-OEt ($\sigma=0.10$).[12] The 15-crown-5 group in **2a** was therefore confirmed as an electron donating 'substituent', similar to *p*-CH$_3$ that has a σ of −0.17.[12] Its CT behavior was hence expected to be similar to that of **1** dominated by the BA-like CT that the amido aniline acted as the electron donor.[5] Although the 15-crown-5 group in **2b** and **2c** would certainly be electron donating as a 'substituent' at the amido aniline, the CT behavior of **2b** and **2c** remains to be clarified because of the increased electron donor strength of the 4-diethylamino and 4-dibutyl-amino groups in **2b** and **2c**, respectively. The latter would enhance the DMABA-like CT in **2b** and **2c** as suggested from the observations made with the CT in a series of 4-(dialkylamino)benzonitriles of lengthening alkyl substituent.[9]

2.2. Intramolecular charge transfer with 2a–c

As the 15-crown-5 group in **2a** was identified as a 'substituent' similar to *p*-CH$_3$, the CT and emission of **2a** would be similar to those of the *p*-CH$_3$ derivative of **1**, **1a** (Chart 1).[5] In a nonpolar solvent such as cyclohexane (CHX) the CT in **2a** would therefore be the BA-like while in highly polar solvents such as acetonitrile (ACN) the BA-like CT is mixed with the DMABA-like, as reported for **1a**.[5] The electron donating ability of the 4-diethylamino and 4-dibutyl-amino groups in **2b** and **2c**, respectively, is stronger than that of the 4-dimethylamino group in **2a**, it was therefore not clear on the CT character of **2b** and **2c**. In order to confirm this hypothesis, fluorescence spectra of **2a–c** and their model molecules **3a–c** (Chart 1) in the following solvents, CHX, diethyl ether (DEE), tetrahydrofuran (THF), dichloromethane (CH$_2$Cl$_2$), and ACN, in an order of increasing polarity, were recorded and compared. Main spectral parameters are summarized in Table 1. Dual fluorescence was observed with **2a–c** in most cases. The fluorescence spectra of **2a** in a variety of solvents are shown in Figure 1 as an example. The long-wavelength emission of **2a** in CHX peaks at 515 nm. This emission in CHX can be reasonably assigned to the BA-like CT state in view of the emission of **1a** in CHX.[5] It is noticeable that the long-wavelength CT emission of **2a** observed in CHX does not undergo an expected monotonous red-shift when the solvent polarity is increased (Fig. 1 and Table 1). As shown in Figure 1, the long-wavelength

Table 1. Absorption and fluorescence spectroscopic parameters of **2a–c** and **3a–c** in organic solvents

	Solvent	Absorption		Fluorescence		
		λ_{abs} (nm)	ε (10^4 L mol^{-1} cm^{-1})[a]	λ_{LE} (nm)	λ_{CT} (nm)	Φ_F[b]
2a	CHX	307	2.27	334.4	515.0	—
	DEE	308	2.85	344.0	400.0	0.0013
	THF	311	3.09	344.0	432.0	0.0025
	CH$_2$Cl$_2$	318	2.73	345.0	451.0	0.0012
	ACN	314	2.78	346.0	495.0	0.0013
2b	CHX	312	2.70	370.0	510.0	0.0041
	DEE	313	3.63	344.0	408.0	0.0020
	THF	316	3.72	348.0	432.0	0.0022
	CH$_2$Cl$_2$	323	3.46	353.0	460.0	0.0021
	ACN	320	3.49	364.0	490.0	0.0016
2c	CHX	314	2.54	370.0	510.0	0.0045
	DEE	314	3.45	346.0	400.0	0.0029
	THF	317	3.48	348.0	429.0	0.0038
	CH$_2$Cl$_2$	325	3.30	353.0	451.0	0.0027
	ACN	321	3.06	356.0	480.0	0.0023
3a	CHX	284/295	0.68/0.59	335.0	—	0.1343
	DEE	285/297	1.53/1.28	342.0	—	0.1734
	THF	290	0.63	347.0	402.0	0.2301
	CH$_2$Cl$_2$	295/300	0.89/0.87	351.0	420.0	0.0801
	ACN	292	0.79	348.0	466.0	0.0806
3b	CHX	290/300	1.29/1.19	338.0	—	0.1053
	DEE	290/298	1.65/1.57	345.0	392.0	0.1250
	THF	294	1.18	350.0	412.0	0.0744
	CH$_2$Cl$_2$	296/307	1.13/1.18	355.0	422.0	0.0988
	ACN	300	0.93	351.0	464.0	0.0758
3c	CHX	288/299	1.79/1.66	342.0	—	0.1009
	DEE	290/300	1.44/1.37	354.0	392.0	0.1146
	THF	295	1.31	358.0	402.0	0.1540
	CH$_2$Cl$_2$	296/308	1.46/1.56	358.0	420.0	0.1603
	ACN	302	1.36	358.0	449.0	0.0944

[a] Mean of three measurements with standard deviation of less than 10%.
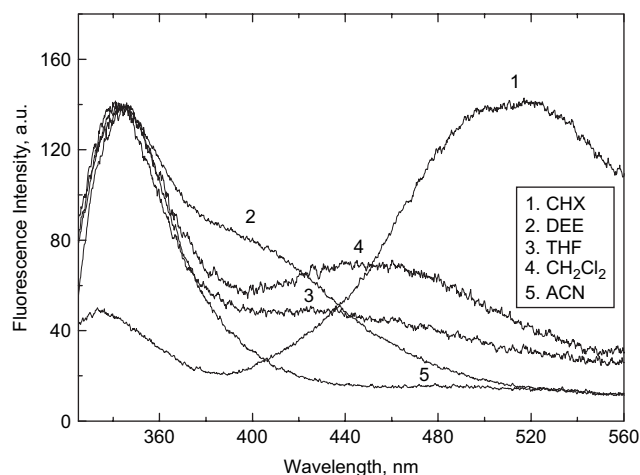[b] Mean of three measurements with standard deviation of less than 30%.

Figure 1. Fluorescence spectra of **2a** in solvents of varied polarity. Solvent: CHX, cyclohexane; DEE, diethyl ether; THF, tetrahydrofuran; CH$_2$Cl$_2$, dichloromethane; and ACN, acetonitrile. [**2a**]=1.00×10^{-5} mol L^{-1}. Excitation wavelength was 290 nm.

band of **2a** shifts dramatically to the blue from 510 nm in CHX to 400 nm in a weakly polar solvent DEE. Upon further increase in solvent polarity (from DEE to THF, CH$_2$Cl$_2$, and ACN), however, it shifts again to the red from 400 nm to 495 nm, indicating again the CT nature of the emissive state in these polar solvents. This apparently 'abnormal' solvatochromism, similar to what was observed with **1a**,[5] confirms that there are two CT channels of opposite direction with **2a** and the CT character changes from purely the BA-like CT in CHX to that mixed by the DMABA-like in polar solvents. Concentration dependent experiments were carried out with **2a** in ACN over 2.0×10^{-6}–1.2×10^{-4} mol L^{-1} and in CHX over 2.0×10^{-6}–1.2×10^{-5} mol L^{-1}. No dependence in the emission spectrum shape was observed. Aggregation that might lead to excimer or exciplex formation, another possible origin for the long-wavelength emission of **2a** particularly in nonpolar solvent CHX, could hence be ruled out. The same conclusion regarding to the CT character can be made with **2b** and **2c** because of the similar solvatochromism observed in their long-wavelength emission.

A comparison of the solvatochromism of the long-wavelength emission of **2a–c** with that of **3a–c**, that have only the DMABA-like CT, supported the conclusion made on the CT character of **2a–c**. Data given in Table 1 indicate that the long-wavelength emission of **3a–c** shifts, as expected for the DMABA-like CT fluorescence,[6] to the red with increasing solvent polarity. It is also observed that the long-wavelength emission of **2a–c** in polar solvent peaks at longer wavelength than that of the corresponding **3a–c**, which indicates the presence of the BA-like CT state of **2a–c**, since the emission from the BA-like CT state appears at longer wavelength in the same solvent than that from the DMABA-like CT state.[7] The fact that the fluorescence quantum yields of **2a–c** are much lower than those of **3a–c** in the same solvent over a large polarity range (Table 1) indicates that the BA-like CT is actually a predominant CT channel with **2a–c** even in highly polar solvents such as ACN. It is hence made clear that compounds **2a–c** have two competitive CT channels of opposite direction. With increasing solvent polarity from CHX to ACN, the CT character in **2**

changes from the BA-like to that of the BA-like dominant with contribution of the DMABA-like CT.

2.3. Compounds 2a–c as the CT dual fluorescent sensors for metal cations

Fluoroionophores **2a–c** as the CT dual fluorescent sensors for alkali and alkaline earth metal cations such as Li$^+$, Na$^+$ K$^+$, Mg^{2+}, Ca^{2+}, and Ba^{2+} were examined in ACN by using both absorption and fluorescence spectroscopy. Detailed spectroscopic data of **2a–c** and their metal complexes in ACN are summarized in Table 2. 15-Crown-5 is known to bind alkali and alkaline earth metal cations. The binding was confirmed by means of NMR titration in **2** by taking Na$^+$/**2a** complex as an example. In the presence of excess amount of Na$^+$, the ^{1}H NMR chemical shifts in DMSO-d_6 of the –CH$_2$ protons of the 15-crown-5 group and the amido –NH proton in **2a** shifted to downfield significantly.[11] Meanwhile, the absorption and fluorescence spectra of **3a–c** (Chart 1), the crown-free model molecules of **2a–c**, showed practically no change in the presence of metal cations. This observation further supports that metal cations bind to the crown-ether group in **2a–c**. It is found in Table 2 that in general the alkaline earth metal cations induce more significant changes in the spectra of **2a–c** than the alkali metal cations. This agrees with the assignment of the binding of metal cation to the crown-ether group in **2a–c**. Figure 2 shows the absorption and fluorescence spectra of **2a–c** in ACN in the presence of Ca^{2+}. It is noted that the absorption spectra of **2a–c** undergo only a slight red-shift by ca. 4 nm in the presence of an excess amount of Ca^{2+} and isosbestic points can be located at 267 nm and 312 nm for **2a**, 271 nm and 319 nm for **2b**, and at 271 nm and 318 nm for **2c**. Similar but smaller red-shift in the absorption spectra of **2a–c** was observed when the other five metal cations were present (Table 2). The red-shifts in the absorption spectra in the presence of metal cations can be explained in terms of the decreased electron-donating character of the 15-crown-5 moiety when a metal cation binds to it.[2a,b] Despite the minor changes in the absorption spectra, the appearance of the isosbestic points in the spectral titration traces point to the formation of well defined complexes between the metal cations and **2a–c**. Job plots (not shown) point to the 1:1 binding stoichiometry.

In contrast, the originally weak fluorescent **2a–c** experience substantial changes in their dual emission when metal cations are introduced (see Fig. 2b for the case of Ca^{2+} and Table 2 for detailed data). It is noted in Figure 2b that, upon introduction of Ca^{2+}, the intensities of the LE and CT emissions are enhanced, despite to different extents, and the LE emission is substantially shifted to the red. Red-shifts of the CT emission bands can also be identified in the presence of metal cation, although they are not as significant as those of the LE emission (see data in Table 2). It is therefore made clear that substantial changes occur in the total fluorescence quantum yield, the CT to LE emission intensity ratio, and the LE band position of **2a–c** in ACN when metal cations bind to their 15-crown-5 moiety. This means that the CT dual fluorescence of **2a–c** can indeed be employed as the sensing parameters for metal cations.

Figures 3–5 display the response profiles against metal cation concentration of the CT emission intensity enhancement

Table 2. Absorption and fluorescence spectroscopic data of **2a–c** and their metal complexes in ACN at room temperature (298 K)

	Absorption		Fluorescence			$\Delta\nu_{ST}$ (cm^{-1})[b]	log K[c]
	λ_{abs} (nm)	ε (10^4 mol^{-1} L cm^{-1})	λ_{LE} (nm)	λ_{CT} (nm)	Φ_{Rel}[a]		
2a	314	3.48	346.0	495.0	1.00	2945.4	—
2a+Li$^+$	317	3.49	349.8	495.0	1.31	2957.9	4.09
2a+Na$^+$	315	3.48	353.8	495.0	1.38	3481.4	4.32
2a+K$^+$	315	3.73	349.0	495.0	1.15	3092.7	3.57
2a+Mg^{2+}	317	3.53	370.0	500.0	5.92	4518.7	5.38
2a+Ca^{2+}	318	3.61	371.0	500.0	6.46	4492.3	5.67
2a+Ba^{2+}	317	3.49	369.0	500.0	3.31	4445.4	5.92
2b	320	3.94	364.0	490.0	1.00	3777.5	—
2b+Li$^+$	321	3.81	367.0	490.0	2.43	3904.6	4.37
2b+Na$^+$	321	3.96	369.0	490.0	3.57	4052.3	4.17
2b+K$^+$	321	3.96	367.0	490.0	1.86	3904.6	3.56
2b+Mg^{2+}	324	4.02	372.0	497.0	22.0	3982.5	5.58
2b+Ca^{2+}	324	4.06	373.0	497.0	22.7	4054.5	5.54
2b+Ba^{2+}	322	3.99	373.0	498.0	12.4	4246.2	5.78
2c	321	3.97	356.0	480.0	1.00	3062.7	—
2c+Li$^+$	322	4.05	366.6	480.0	2.25	3778.2	4.32
2c+Na$^+$	322	3.98	370.0	480.0	3.19	4028.9	4.35
2c+K$^+$	321	3.94	365.6	480.0	2.00	3800.3	3.49
2c+Mg^{2+}	324	4.08	379.0	483.0	18.5	4479.0	5.33
2c+Ca^{2+}	324	4.09	378.0	482.0	19.6	4409.2	5.31
2c+Ba^{2+}	323	4.00	378.0	480.0	8.31	4504.8	5.90

[a] Quantum yield relative to that of sensor; metal cation concentration is 100 times that of the sensor's.
[b] Stokes shift of the LE emission, $\Delta\nu_{ST}=\nu_{abs}-\nu_{flu\,(LE)}$.
[c] Binding constant K in mol^{-1} L.

(I/I_0), the LE band position, and the CT to LE emission intensity ratio of **2a–c**. Note that all of the three parameters increase initially with metal cation concentration and level off at higher metal cation concentration. The corresponding leveled-off parameters can therefore attribute to those of the **2**-metal binding complexes.

Analysis of the variations of these parameters helps to understand the mechanism how the dual fluorescence of **2a–c** responds to the metal cations. It was shown[5] that with **1** the

fluorescence quantum yield increased when the substituent X at the amido aniline phenyl ring became more electron-withdrawing. The quantum yields of **2a–c** increased in the presence of metal cations, in particular of Ca^{2+} with which enhancements of the quantum yields of **2a–c** amounted to 6, 23, and 20 folds (Table 2). The enhancements in the CT emission are more dramatic, being 11, 26, and 21 folds (Fig. 3). With other metal cations dramatic enhancements in the total quantum yields and the CT emission were also found (Fig. 3 and Table 2). Such significant fluorescence
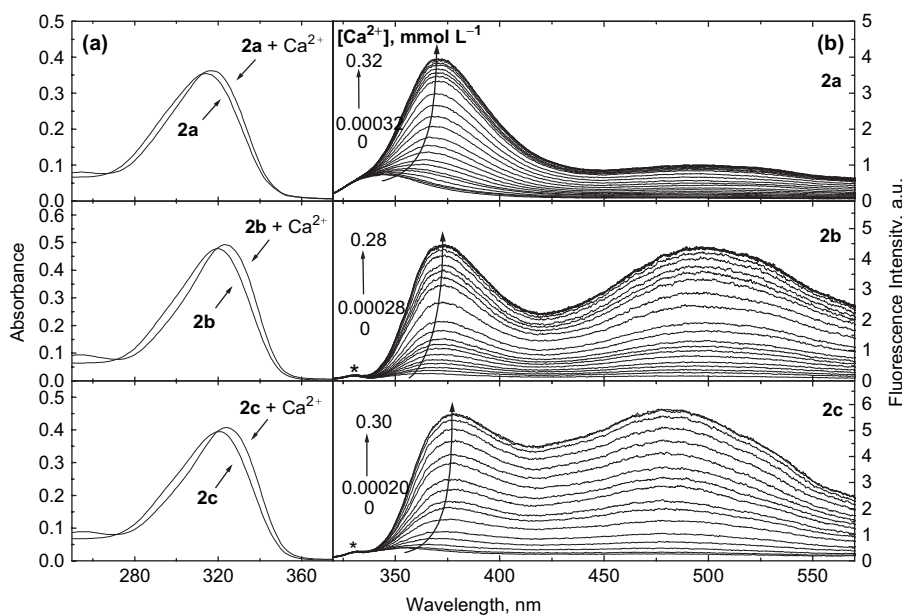

Figure 2. Absorption (a) and fluorescence spectra (b) of **2a** (1.00×10^{-5} mol L^{-1}), **2b** (1.22×10^{-5} mol L^{-1}), and **2c** (1.00×10^{-5} mol L^{-1}) in ACN in the absence and the presence of excess amount of Ca^{2+} (a) and of increasing concentration of Ca^{2+} (b). All metal cations existed in the form of perchlorate. Excitation wavelength was 300 nm. Asterisks in (b) refer to Raman scattering.
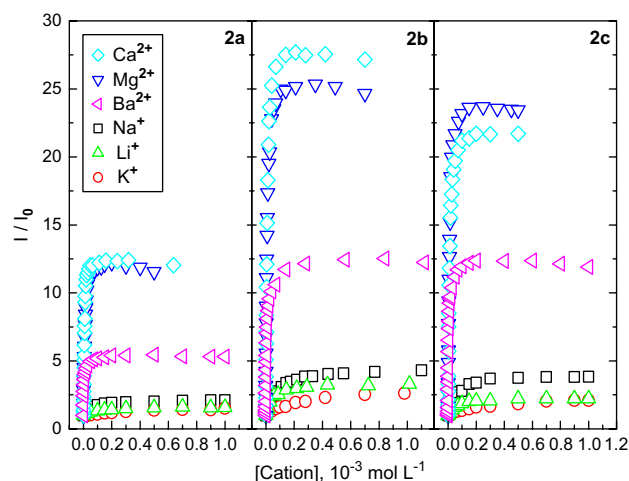
Figure 3. The CT fluorescence intensity enhancement (I/I_0) of **2a–c** as a function of cation concentration. Excitation wavelength was 300 nm. I and I_0 represent the CT emission intensities in the presence and absence of the metal cation, respectively.

enhancements have only been observed in some of the PET fluorescent sensing systems[13] and several well-designed ICT systems.[10]

The red-shift of the LE band of **2a–c** in ACN in the presence of metal cations is very helpful for understanding the emission enhancement. As shown in Figure 4, Mg^{2+}, Ca^{2+}, and Ba^{2+} induce substantial red-shifts in the LE emission (see also $\Delta\nu_{ST}$ in Table 2), whereas the monovalent alkali metal cations, Li^+, Na^+, and K^+ result in relatively less red-shifts. Upon comparing the LE band positions of the **2a**-metal complexes with those of **1** derivatives,[5] it was found that the LE band of **2a** that originally peaked at 346 nm was close to the LE band of a derivative of **1** bearing a highly electron-donating substituent. It shifted to 371 nm in its complex with Ca^{2+} that bears an analogy to a derivative of **1** with an electron-withdrawing substituent, *p*-Cl (Fig. 4). Obviously, cation binding changes the nature of the 15-crown-5 moiety in **2a**, considered as a substituent at the amido aniline of **1**,
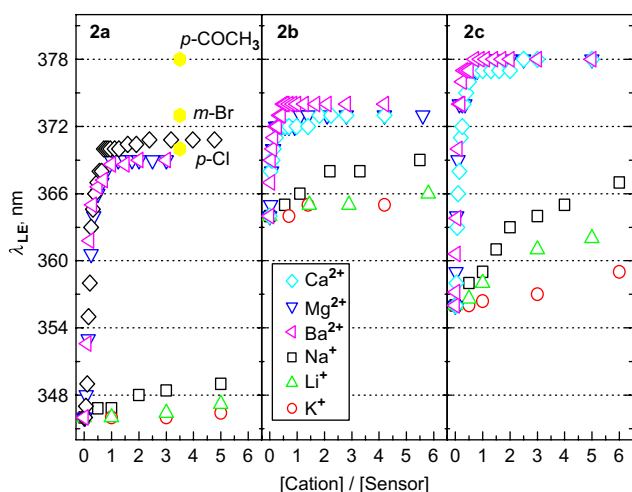

Figure 4. The LE band positions of **2a–c** in ACN in the presence of metal perchlorates. Excitation wavelength was 300 nm. Solid hexahedral symbols are the LE band position data taken from [5] for the derivatives of **1** bearing the indicated substituents at the amido aniline.
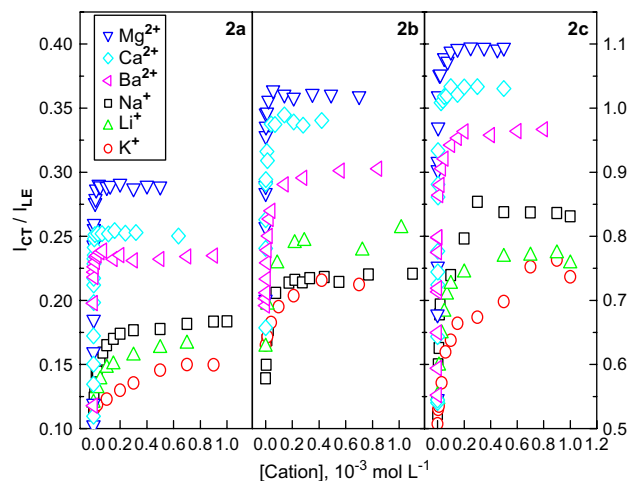

Figure 5. Plots of the CT to LE fluorescence intensity ratios of **2a–c** versus cation concentration. Plots of **2a** have the left coordinate and those of **2b** and **2c** have the same right coordinate.

from electron donating to withdrawing. This means that **2a**, upon Ca^{2+} binding, changes its structural pattern from D–A–D′ to D–A–A′, the CT occurring in **2a**-Ca^{2+} complex might now be the DMABA-like that the 4-dimethylamino group is the electron donor. For the sake of clarity, part of the previously reported LE band positions of the derivatives of **1** in ACN are also given as solid hexahedrons in Figure 4. The red-shift in the LE band positions of **2b** and **2c** induced by cation binding behaves similar to that of **2a**. For example, the LE emission of **2b** shifts upon binding to Ca^{2+} from 364 to 373 nm and of **2c** from 356 nm to 378 nm.

The LE band positions of the **2b**-Ca^{2+} and **2c**-Ca^{2+} complexes can be compared to those of **1** bearing substituents *m*-Br and *p*-COCH₃, respectively, Figure 4. This means that, in the **2**-Ca^{2+} complexes, the consequence of lengthening the alkyl chain in the 4-dialkylamino group in **2** from methyl (**2a**) to ethyl (**2b**) and *n*-butyl (**2c**) is the same as in **1** with increasing electron-withdrawing ability of the substituent (X) at its amido aniline. It is therefore concluded that in the **2**-metal complexes, the excited-state CT occurs with the 4-dialkylamino group being the electron donor, i.e., the CT in the complexes is the DMABA-like. The 15-crown-5 moiety in **2**, the metal cation binding site, is therefore shown to be within the electron acceptor of their metal complexes. This means that metal cation binding to the crown-ether moiety in **2** results in the switching of the CT from mainly the BA-like with **2** to the DMABA-like with their metal complexes. During such a switching, the BA-like CT emission would be blue shifted while the DMABA-like CT emission is red shifted. This explains the observed small apparent red-shift of the CT emission of **2a–c** upon metal binding (Fig. 2 and Table 2), and in part the increase in the total fluorescence quantum yields of **2a–c** (Table 2).

Variations of the CT to LE emission intensity ratio of **2a–c** with metal cation concentration (Fig. 5) not only confirm that ratiometric fluorescent assays can be established, but they also provide further supports for the conclusion that metal cation binding induces switching of the CT direction in **2a–c**. For example, the observation that the CT to LE emission intensity ratio of the **2**-metal complexes increases
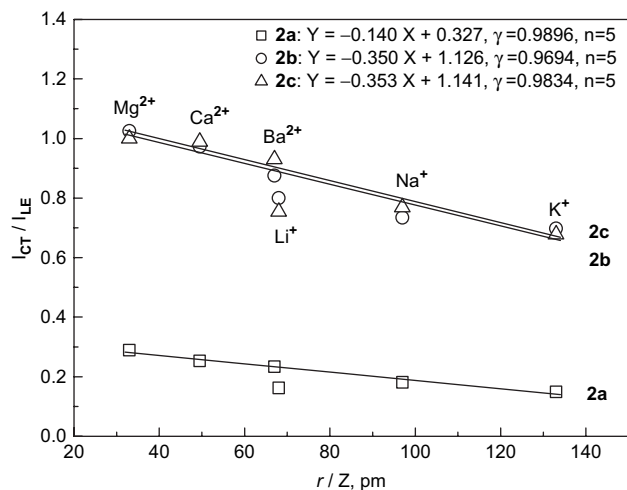
Figure 6. Linear correlation of the CT to LE intensity ratio of the **2**-metal complex with the radius to charge ratio of the metal cation. Data points for Li$^+$ were not included in the linear correlation.

from 0.26 (**2a**+Ca^{2+}) via 0.97 (**2b**+Ca^{2+}) to 0.99 (**2c**+Ca^{2+}) is similar to what was observed with the known CT fluorophores 4-(dialkylamino)benzonitriles of increasing alkyl chain in which the dialkylamino group was identified as the electron donor.[9] Significantly, the CT to LE emission intensity ratio of the metal complexes of **2a–c** was found to show a linear correlation with the charge density parameter (radius to charge ratio, r/Z) of the metal cation Na$^+$, K$^+$, Mg^{2+}, Ca^{2+}, and Ba^{2+},[14] with Li$^+$ being off line[15] (Fig. 6). This observation indicates that the electronic attractive interaction between the metal cation and the crown-ether moiety in **2a–c** promotes the total DMABA-like CT in the complex,[14c] confirming that the crown-ether moiety is within the electron acceptor of the complex. The observed linear slopes of the metal complexes of **2a–c** vary in the order of **2c**∼**2b**>**2a** of decreasing electron donating ability of the 4-dialkylamino group in **2** indicates that the metal cation influence is stronger in case where more DMABA-like CT is expected. This suggests that in the metal complexes of **2a–c** the occurrence of the DMABA-like CT enhances the metal cation binding to **2a–c**.

2.4. Binding constants of 2a–c with metal cations

Binding constants of **2a–c** with the investigated metal cations in ACN were then evaluated by nonlinear regressions[16] from the fluorescence titration data. The data can be nicely fitted assuming a 1:1 binding stoichiometry, which is confirmed by the Job plots (not shown). The log K values of **2a–c** differ not much with the same cation, while for the same sensor they vary in the order of Mg^{2+}∼Ca^{2+}∼Ba^{2+}>Na$^+$∼Li$^+$>K$^+$ (Table 2). The latter order is again consistent with the electronic attractive nature for the interaction between metal cation and the crown-ether moiety in **2**. The binding constants of the metal cations with **2** were found indeed higher than those with ionophores bearing benzo-15-crown-5 binding moiety but without the occurrence of the excited-state CT[13b,17] and, in particular, higher than those with the CT dual fluorescent sensors with the aza-15-crwon-5 binding site being within the electron donor.[2a–d,2h,3b,10b,c,15] The high binding constants for alkaline metal cations at 10^5 mol^{-1} L orders of magnitude

(Table 2) make highly sensitive ratiometric fluorescent assays possible at sub-micromolar level (Figs. 2 and 5).

3. Conclusions

A series of the CT dual fluorescent sensors **2a–c** for alkali and alkaline earth metal cations with cation binding site within the electron acceptor were developed. These sensors were designed on the basis of the structural framework of 4-(dimethylamino)benzanilides (**1**) in which two CT channels of opposite direction were identified by varying the substituents at the amido aniline phenyl ring. 15-Crown-5 was incorporated in but separated from the amide moiety by a rigid phenyl ring, thereby avoiding any steric consequence when the metal cation binds to the 15-crown-5 moiety. Indeed, **2a–c** underwent substantial changes in their CT photophysics and the accompanied dual emission upon metal cation binding in ACN, i.e., increased total quantum yield and the CT to LE emission intensity ratio, and the red-shifted LE emission. These changes were shown to result from the switching of the CT character of mainly the BA-like in the absence of the metal cation to the DMABA-like when metal cation bound to the 15-crown-5 moiety. We therefore succeeded in developing the CT dual fluorescent sensors for cations with binding site within the electron acceptor and without obvious steric interference caused by cation binding. The expected CT-facilitated cation binding was confirmed by the higher cation binding constants. Substantial increase in the CT to LE emission intensity ratio upon cation binding also allows for highly sensitive ratiometric assays for cations, at for example sub-micromolar level for the alkaline metal cations. As a wealth of knowledge is now available with the related CT photophysics,[1] and the ease of incorporating other metal binding groups in the amido aniline phenyl ring, extensions of the current proof-of-principle structural framework are promising in constructing CT dual fluorescent sensors for metals of better and more practical applications.

4. Experimental

4.1. Instruments

Steady-state fluorescence spectra were recorded with a Hitachi F-4500 fluorescence spectrophotometer using excitation and emission slits of 5 nm. Fluorescence quantum yields were measured using quinine sulfate as a standard (Φ_F= 0.546 in 0.5 mol L^{-1}).[18] Absorption spectra were taken on a Varian Cary 300 absorption spectrophotometer using a 1-cm quartz cell. ^{1}H NMR (500 MHz) and ^{13}C NMR (125 MHz) data were acquired in CDCl$_3$ on a Varian Unity$^+$ 500 MHz NMR spectrometer using TMS as an internal reference. HRMS were obtained on a Micromass LCT spectrometer. Elemental analyses were carried out by using CARLO ERBA1500 element analyzer.

4.2. Materials

4-(Dimethylamino)benzoic acid was synthesized from the reaction of 4-aminobenzoic acid with dimethylsulfate in alkaline aqueous solution.[19] 4-(Diethylamino)benzoic acid was purchased from Aldrich. 4-(Di(*n*-butyl)amino)benzoic

acid was synthesized according to a reported method.[20] Alkali and alkaline earth metal perchlorates were purchased from Shanghai Chemicals Company (Shanghai, China) and were kept anhydrous over P_2O_5 in a desiccator. Solvents for spectroscopic measurements were purified before use and checked to have no fluorescent impurity at the employed excitation wavelengths.

4.3. General procedures for the synthesis of 2a–c and 3a–c

As shown in Scheme 1, **2a–c** were synthesized by addition of 4-(dialkylamino)benzoyl chloride into CH_2Cl_2 solution of 4-aminobenzo-15-crown-5 hydrochloride and triethylamine, followed by stirring at room temperature for 6 h. The crude products were purified by column chromatography on silica gel by using CH_2Cl_2, ethyl acetate, and methanol mixture (8:1:1, v/v/v) as the eluent. The model molecules **3a–c** were synthesized in a similar manner and the crude products were easily obtained by removing the solvent and by washing with dilute aqueous NaOH solution. The obtained white precipitates were purified by repeated recrystallizations from acetone.

4.3.1. 4-Dimethylamino-N-(6,7,9,10,12,13,15,16-octahydro-5,8,11,14,17-pentaoxabenzocyclopentadecen-2-yl)-benzamide (2a).
^{1}H NMR (CDCl$_3$, 500 MHz) δ 3.03 (s, 6H), 3.75 (d, J=4.5 Hz, 8H), 3.88–3.91 (m, 4H), 4.12 (t, J=4 Hz, 2H), 4.15 (t, J=4 Hz, 2H), 6.71 (d, J=8.5 Hz, 2H), 6.83 (d, J=8.5 Hz, 1H), 6.95 (d, J=8.5 Hz, 1H), 7.52 (s, 1H), 7.77 (d, J=8.5 Hz, 2H), 7.82 (s, 1H) ppm. ^{13}C NMR (CDCl$_3$, 125 MHz) δ 40.27 (2C), 68.69 (1C), 69.44 (1C), 69.69 (2C), 70.39 (1C), 70.58 (1C), 70.92 (1C), 71.01 (1C), 107.18 (1C), 111.43 (2C), 112.41 (1C), 114.89 (1C), 121.81 (1C), 128.56 (2C), 132.88 (1C), 145.44 (1C), 149.35 (1C), 152.27 (1C), 165.46 (O=C) ppm. HRMS (ESI) for $C_{23}H_{31}N_2O_6$ (M+H$^+$) calcd 431.2182, found 431.2183 (M+H$^+$), 453.2003 (M+Na$^+$). Anal. Calcd for $C_{23}H_{30}N_2O_6$: C, 64.17; H, 7.02; N, 6.51. Found: C, 64.04; H, 6.95; N, 6.30.

4.3.2. 4-Diethylamino-N-(6,7,9,10,12,13,15,16-octahydro-5,8,11,14,17-pentaoxabenzocyclopentadecen-2-yl)benz-amide (2b).
^{1}H NMR (CDCl$_3$, 500 MHz): 1.19 (t, J=7 Hz, 6H), 3.38–3.42 (m, 4H), 3.75 (d, J=4 Hz, 8H), 3.87–3.90 (m, 4H), 4.12 (t, J=4 Hz, 2H), 4.15 (t, J=4 Hz, 2H), 6.65 (s, 2H), 6.82 (d, J=8.5 Hz, 1H), 6.94 (d, J=7 Hz, 1H), 7.52 (s, 1H), 7.75 (d, J=8 Hz, 2H), 7.80 (s, 1H) ppm. ^{13}C NMR (CDCl$_3$, 125 MHz): 12.41 (2C), 44.40 (2C), 68.66 (1C), 69.43 (1C), 69.68 (2C), 70.38 (1C), 70.57 (1C), 70.91 (1C), 71.01 (1C), 107.05 (1C), 110.47 (2C), 112.27 (1C), 114.89 (1C), 120.27 (1C), 128.79 (2C), 132.91 (1C), 145.35 (1C), 149.33 (1C), 150.16 (1C), 165.39 (O=C) ppm. HRMS (ESI) for $C_{25}H_{35}N_2O_6$ calcd 459.2495 (M+H$^+$), found 459.2495 (M+H$^+$), 481.2351 (M+Na$^+$). Anal. Calcd for $C_{25}H_{34}N_2O_6$: C, 65.48; H, 7.47; N, 6.11. Found: C, 65.66; H, 7.81; N, 5.86.

4.3.3. 4-Dibutylamino-N-(6,7,9,10,12,13,15,16-octahydro-5,8,11,14,17-pentaoxabenzocyclopentadecen-2-yl)benz-amide (2c).
^{1}H NMR (CDCl$_3$, 500 MHz): 0.96 (t, J=7 Hz, 6H), 1.34–1.39 (m, 4H), 1.58 (s, 4H), 3.31 (t, J=7.5 Hz, 4H), 3.75 (d, J=4 Hz, 8H), 3.89 (s, 4H), 4.11 (t, J=4 Hz, 2H), 4.15 (t, J=4 Hz, 2H), 6.62 (s, 2H), 6.83 (d, J=8.5 Hz, 1H), 6.91 (d, J=7.5 Hz, 1H), 7.52 (s, 1H), 7.72 (s, 3H) ppm. ^{13}C NMR (CDCl$_3$, 125 MHz): 13.91 (2C), 20.22 (2C), 29.22 (2C), 50.68 (2C), 68.66 (1C), 69.43 (1C), 69.70 (2C), 70.38 (1C), 70.55 (1C), 70.91 (1C), 70.99 (1C), 107.03 (1C), 110.57 (2C), 112.22 (1C), 114.91 (1C), 120.15 (1C), 128.69 (2C), 132.93 (1C), 145.33 (1C), 149.35 (1C), 150.57 (1C), 165.39 (O=C) ppm. HRMS (ESI) for $C_{29}H_{43}N_2O_6$ calcd 515.3121 (M+H$^+$), found 515.3116 (M+H$^+$), 537.2929 (M+Na$^+$). Anal. Calcd for $C_{29}H_{42}N_2O_6$: C, 67.68; H, 8.23; N, 5.44. Found: C, 67.36; H, 8.12; N, 5.28.

4.3.4. 4-Dimethylamino-N-(iso-propyl)benzamide (3a).
^{1}H NMR (CDCl$_3$, 500 MHz): 1.24 (d, J=6.5 Hz, 6H), 3.00 (s, 6H), 4.23–4.32 (m, 1H), 5.85 (s, 1H), 6.66 (d, J=8 Hz, 2H), 7.67 (d, J=9 Hz, 2H) ppm. ^{13}C NMR (CDCl$_3$, 125 MHz): 22.95 (2C), 40.14 (2C), 41.48 (1C), 111.09 (2C), 121.83 (1C), 128.19 (2C), 152.22 (1C), 166.56 (O=C) ppm. HRMS (ESI) for $C_{12}H_{19}N_2O$ calcd 207.1497 (M+H$^+$), found 207.1495. Anal. Calcd for $C_{12}H_{18}N_2O$: C, 69.87; H, 8.80; N, 13.58. Found: C, 69.68; H, 9.00; N, 13.72.

4.3.5. 4-Diethylamino-N-(iso-propyl)benzamide (3b).
^{1}H NMR (CDCl$_3$, 500 MHz): 1.17 (t, J=7 Hz, 6H), 1.23 (d, J=6.5 Hz, 6H), 3.36–3.40 (m, 4H), 4.23–4.32 (m, 1H), 5.80 (s, 1H), 6.62 (d, J=8.5 Hz, 2H), 7.64 (d, J=9 Hz, 2H) ppm. ^{13}C NMR (CDCl$_3$, 125 MHz): 12.43 (2C), 22.99 (2C), 41.42 (1C), 44.38 (2C), 110.42 (2C), 120.77 (1C), 128.47 (2C), 149.82 (1C), 166.56 (O=C) ppm. HRMS (ESI) for $C_{14}H_{23}N_2O$ calcd 235.1810 (M+H$^+$), found 235.1808. Anal. Calcd for $C_{14}H_{22}N_2O$: C, 71.76; H, 9.46; N, 11.95. Found: C, 71.90; H, 9.38; N, 12.19.

4.3.6. 4-Dibutylamino-N-(iso-propyl)benzamide (3c).
^{1}H NMR (CDCl$_3$, 500 MHz): 0.95 (t, J=7.5 Hz, 6H), 1.23 (d, J=6.5 Hz, 6H), 1.31–1.39 (m, 4H), 1.53–1.59 (m, 4H), 3.29 (t, J=7.5 Hz, 4H), 4.22–4.32 (m, 1H), 5.80 (s, 1H), 6.58 (d, J=8.5 Hz, 2H), 7.63 (d, J=8.5 Hz, 2H) ppm. ^{13}C NMR (CDCl$_3$, 125 MHz): 13.89 (2C), 20.20 (2C), 22.97 (2C), 29.21 (2C), 41.36 (1C), 50.63 (2C), 110.44 (2C), 120.58 (1C), 128.35 (2C), 150.19 (1C), 166.54 (O=C) ppm. HRMS (ESI) for $C_{18}H_{31}N_2O$ calcd 291.2436 (M+H$^+$), found 291.2441. Anal. Calcd for $C_{18}H_{30}N_2O$: C, 74.44; H, 10.41; N, 9.65. Found: C, 73.96; H, 10.38; N, 9.24.

References and notes

1. (a) Grabowski, Z. R.; Rotkiewicz, K.; Siemiarczuk, A.; Cowley, D. J.; Baumann, W. *Nouv. J. Chim.* **1979**, *3*, 443; (b) Rettig, W. *Angew. Chem., Int. Ed. Engl.* **1986**, *25*, 971; (c) Grabowski, Z. R.; Rotkiewicz, K.; Rettig, W. *Chem. Rev.* **2003**, *103*, 3899.

2. (a) Fery-Forgues, S.; Le Bris, M.-T.; Guetté, J.-P.; Valeur, B. *J. Phys. Chem.* **1988**, *92*, 6233; (b) Bourson, J.; Valeur, B. *J. Phys. Chem.* **1989**, *93*, 3871; (c) Létard, J.-F.; Lapouyade, R.; Rettig, W. *Pure Appl. Chem.* **1993**, *65*, 1705; (d) Létard, J.-F.; Delmond, S.; Lapouyade, R.; Braun, D.; Rettig, W. *Recl. Trav. Chim. Pays-Bas* **1995**, *114*, 517; (e) Collins, G. E.; Choi, L.-S.; Callahan, J. H. *J. Am. Chem. Soc.* **1998**, *120*, 1474; (f) Choi, L.-S.; Collins, G. E. *Chem. Commun.* **1998**, 893; (g) Marcotte, N.; Plaza, P.; Lavabre, D.; Fery-Forgues, S.; Martin, M. M. *J. Phys. Chem. A* **2003**, *107*, 2394; (h) Yang, J.-S.; Hwang, C.-Y.; Hsieh, C.-C.; Chiou, S.-Y. *J. Org. Chem.* **2004**, *69*, 719.

3. (a) Martin, M. M.; Plaza, P.; Dai Hung, N.; Meyer, Y. H.; Bourson, J.; Valeur, B. *Chem. Phys. Lett.* **1993**, *202*, 425; (b) Dumon, P.; Jonusauskas, G.; Dupuy, F.; Pée, P.; Rullière, C.; Létard, J.-F.; Lapouyade, R. *J. Phys. Chem.* **1994**, *98*, 10391; (c) Mathevet, R.; Jonusauskas, G.; Rullière, C.; Létard, J.-F.; Lapouyade, R. *J. Phys. Chem.* **1995**, *99*, 15709; (d) Martin, M. M.; Plaza, P.; Meyer, Y. H.; Badaoui, F.; Bourson, J.; Lefèvre, J.-P.; Valeur, B. *J. Phys. Chem.* **1996**, *100*, 6879; (e) Plaza, P.; Leray, I.; Changenet-Barret, P.; Martin, M. M.; Valeur, B. *ChemPhysChem* **2002**, *3*, 668.

4. (a) Malval, J.-P.; Lapouyade, R. *Helv. Chim. Acta* **2001**, *84*, 2439; (b) Malval, J.-P.; Lapouyade, R.; Léger, J.-M.; Jarry, C. *Photochem. Photobiol. Sci.* **2003**, *2*, 259.

5. Zhang, X.; Wang, C.-J.; Liu, L.-H.; Jiang, Y.-B. *J. Phys. Chem. B* **2002**, *106*, 12432.

6. Braun, D.; Rettig, W.; Delmond, S.; Letard, J.-F.; Lapouyade, R. *J. Phys. Chem. A* **1997**, *101*, 6836.

7. (a) Heldt, J.; Gormin, D.; Kasha, M. *J. Am. Chem. Soc.* **1988**, *110*, 8255; (b) Heldt, J.; Gormin, D.; Kasha, M. *Chem. Phys. Lett.* **1988**, *150*, 433; (c) Heldt, J.; Heldt, J. R.; Szatan, E. *J. Photochem. Photobiol. A: Chem.* **1999**, *121*, 91; (d) Lewis, F. D.; Long, T. M. *J. Phys. Chem. A* **1998**, *102*, 5327; (e) Zhang, X.; Sun, X.-Y.; Wang, C.-J.; Jiang, Y.-B. *J. Phys. Chem. A* **2002**, *106*, 5577.

8. Huang, W.; Zhang, X.; Ma, L.-H.; Wang, C.-J.; Jiang, Y.-B. *Chem. Phys. Lett.* **2002**, *352*, 401.

9. (a) Schuddeboom, W.; Jonker, S. A.; Warman, J. M.; Leinhos, U.; Kühnle, W.; Zachariasse, K. A. *J. Phys. Chem.* **1992**, *96*, 10809; (b) Il'ichev, Y.; Kühnle, W.; Zachariasse, K. A. *J. Phys. Chem. A* **1998**, *102*, 5670.

10. (a) Crochet, P.; Malval, J.-P.; Lapouyade, R. *Chem. Commun.* **2000**, 289; (b) Rurack, K.; Rettig, W.; Resch-Genger, U. *Chem. Commun.* **2000**, 407; (c) Rurack, K.; Koval'chuck, A.; Bricks, J. L.; Slominskii, J. L. *J. Am. Chem. Soc.* **2001**, *123*, 6205.

11. ¹H NMR data (in ppm) of **2a** in DMSO-d_6 in the absence and the presence of saturated NaClO$_4$: (a) **2a** in the absence of NaClO$_4$, 2.995 (s, 6H), 3.617 (s, 8H), 3.759–3.788 (m, 4H), 4.023 (s, 4H), 6.749 (d, *J*=9 Hz, 2H), 6.898 (d, *J*=8.5 Hz, 1H), 7.279 (d, *J*=8.5 Hz, 1H), 7.462 (s, 1H), 7.845 (d, *J*=8.5 Hz, 2H), and 9.722 (s, 1H); (b) **2a** in the presence of saturated NaClO$_4$, the data becoming 2.996 (s, 6H), 3.635 (s, 8H), 3.777–3.810 (m, 4H), 4.076 (s, 4H), 6.751 (d, *J*=9 Hz, 2H), 6.976 (d, *J*=8.5 Hz, 1H), 7.306 (d, *J*=8.5 Hz, 1H), 7.541 (s, 1H), 7.847 (d, *J*=8.5 Hz, 2H), and 9.760 (s, 1H).

12. Hansch, C.; Leo, A.; Taft, R. W. *Chem. Rev.* **1991**, *91*, 165.

13. (a) de Silva, A. P.; Gunaratne, H. Q. N.; Maguire, G. E. M. *J. Chem. Soc., Chem. Commun.* **1994**, 1213; (b) de Silva, A. P.; Gunaratne, H. Q. N.; McCoy, C. P. *J. Am. Chem. Soc.* **1997**, *119*, 7891; (c) de Silva, A. P.; Gunaratne, H. Q. N.; Gunnlaugsson, T.; Huxley, A. J. M.; McCoy, C. P.; Rademacher, J. T.; Rice, T. E. *Chem. Rev.* **1997**, *97*, 1515; (d) de Silva, A. P.; McClenaghan, N. D. *J. Am. Chem. Soc.* **2000**, *122*, 3965; (e) Ramachandram, B.; Saroja, G.; Sankaran, N. B.; Samanta, A. *J. Phys. Chem. B* **2000**, *104*, 11824; (f) Bag, B.; Bharadwaj, P. K. *J. Phys. Chem. B* **2005**, *109*, 4377.

14. (a) Hall, C. D.; Sharpe, N. W.; Danks, I. P.; Sang, Y. P. *J. Chem. Soc., Chem. Commun.* **1989**, 419; (b) Bourson, J.; Pouget, J.; Valeur, B. *J. Phys. Chem.* **1993**, *97*, 4552; (c) Huang, H.; Mu, L.-J.; He, J.-Q.; Cheng, J.-P. *J. Org. Chem.* **2003**, *68*, 7605.

15. Rurack, K.; Bricks, J. L.; Reck, G.; Radeglia, R.; Resch-Genger, U. *J. Phys. Chem. A* **2000**, *104*, 3087.

16. (a) Connors, K. A. Binding Constants. In *The Measurement of Molecular Complex Stability*; Wiley: New York, NY, 1987; (b) Valeur, B.; Pouget, J.; Bouson, J.; Kaschke, M.; Ernsting, N. P. *J. Phys. Chem.* **1992**, *96*, 6545.

17. (a) Izatt, R. M.; Pawlak, K.; Bradshaw, J. S.; Bruening, R. L. *Chem. Rev.* **1991**, *91*, 1721; (b) Yam, V. W.-W.; Lu, X.-X.; Ko, C.-C. *Angew. Chem., Int. Ed.* **2003**, *42*, 3385; (c) Lu, X.-X.; Li, C.-K.; Cheng, E. C.-C.; Yam, V. W.-W. *Inorg. Chem.* **2004**, *43*, 2225.

18. Demas, J. N.; Crobys, G. A. *J. Phys. Chem.* **1971**, *75*, 991.

19. Jiang, Y.-B. *J. Photochem. Photobiol. A: Chem.* **1994**, *78*, 205.

20. Markovitsi, D.; Jallabert, C.; Strzelecka, H.; Veber, M. *J. Chem. Soc., Faraday Trans.* **1990**, *86*, 2819.